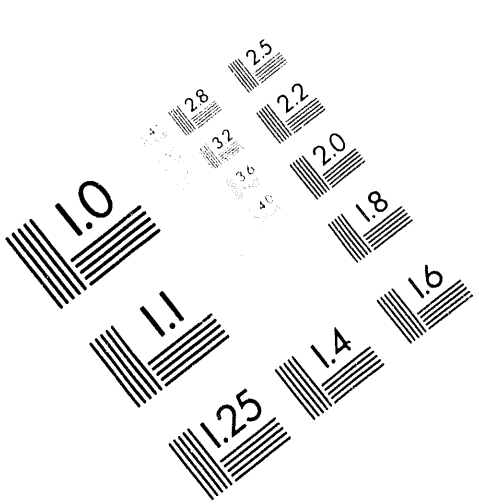

Association for Information and Image Management

1100 Wayne Avenue, Suite 1100
Silver Spring, Maryland 20910

301/587-8202

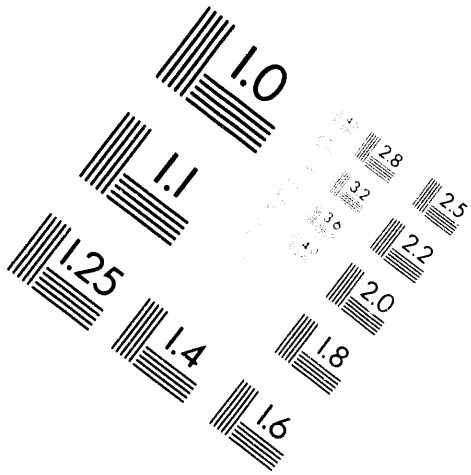

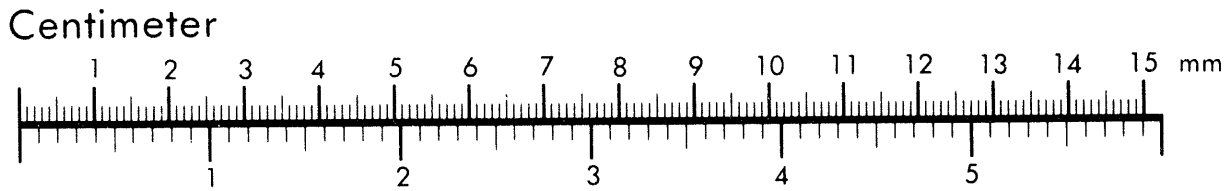

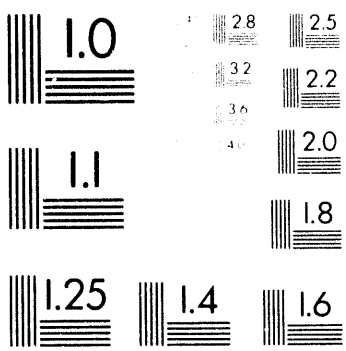

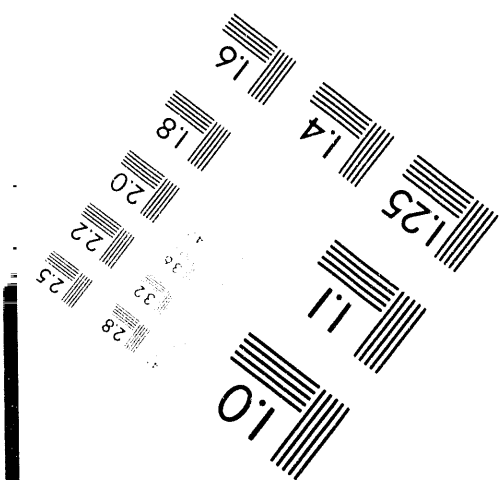

MANUFACTURED TO AIIM STANDARDS
BY APPLIED IMAGE, INC.

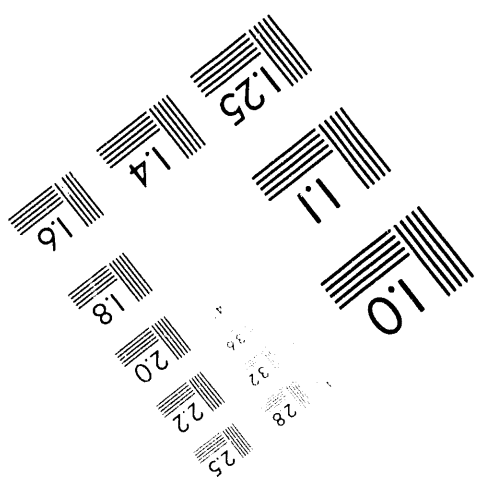

1 of 1

INSTITUTE FOR FUSION STUDIES

DE-FG05-80ET-53088-654 IFSR #654

Isotope Scaling and η_i Mode with Impurities in Tokamak Plasmas

J.Q. DONG,[a] W. HORTON, and W.D. DORLAND
Institute for Fusion Studies
The University of Texas at Austin
Austin, Texas 78712

April 1994

[a]permanent address: Southwestern Institute of Physics, Chengdu, China

THE UNIVERSITY OF TEXAS

AUSTIN

Isotope Scaling and η_i Mode with Impurities in Tokamak Plasmas

J.Q. Dong,[a] W. Horton, and W.D. Dorland
Institute for Fusion Studies
The University of Texas at Austin
Austin, Texas 78712

Abstract

The ion temperature gradient driven instability, or η_i mode, is studied for discharges with hydrogen, deuterium or tritium in a toroidal magnetic configuration. Impurity effects on the mode and the instability which is driven by the presence of impurity ions (impurity modes) are studied as well. It is found that the maximum growth rate of the η_i mode scales as $M^{-\frac{1}{2}}$ for pure hydrogen, deuterium or tritium discharges, where M is the mass of the working gas ion. With the inclusion of impurity ions the growth rates of η_i mode decrease in all three kinds of plasmas with a hydrogen plasma still having the highest maximum growth rate, tritium the lowest, and deuterium in between. However, the isotope effects are weaker and scale as $M_{\rm eff}^{-\frac{1}{2}}$ with the presence of impurity ions, where the effective mass $M_{\rm eff}$ is a combination of A_i and A_z, the mass number of hydrogenic and impurity ions. For the impurity mode the situation is similar to that of the η_i mode without impurity ions. Experimental database shows that the plasma energy confinement time scales as $\tau_E \sim A_i^{\frac{1}{2}}$ in clean plasmas. The correlation of the theoretical results with the experimental confinement scaling is discussed.

---

[a] Permanent address: Southwestern Institute of Physics, Chengdu, China

I Introduction

Obtaining and understanding scaling laws for the energy confinement time in tokamak plasmas have long been one of the focuses of experimental and theoretical studies in fusion plasma physics. Several empirical scaling laws have been proposed and work well for L-mode as well as H-mode discharges.[1, 2, 3] One of the common features of these scaling laws is that the plasma energy confinement time $\tau_E \propto A_i^\alpha$, where A_i is the ion mass number and $0.3 < \alpha < 0.7$ is a constant that varies from one scaling law to another. This τ_E versus A_i^α scaling is called the isotope scaling or isotope effects. Recently, the results of a wide range of studies about the isotope scaling performed on ASDEX as well as on other tokamak devices are reported and a variety of isotope scaling laws obtained from experiments are summarized.[3] Despite its fundamental nature and widespread appearance in the experimental observations, theoretical explanations for the isotope scaling are rare. Moreover, conventional transport theories usually fail in predicting the right isotope scaling. Neoclassical theory, conventional ion pressure gradient driven turbulence models, and resistive ballooning theory, for instance, predict a degradation of confinement from hydrogen to deuterium.

Theoretical attempts have been made to overcome the contradiction between experiments and theories. Impurity ion species are introduced into the ion temperature gradient (ITG) mode turbulence, which is widely believed to be responsible for anomalous energy transport in tokamak plasmas, to make A_i an explicit parameter in the transport properties.[4-6] In addition, the impurity mode which is driven by the presence of second ion species even without ion temperature gradient is considered to account for the energy transport in plasma periphery.[5, 6] A slab magnetic configuration is usually used and even a simplified local dispersion equation valid for long wavelength approximation and shearless slab geometry is solved in these earlier studies. A more complete toroidal equation including ion curvature and mag-

netic gradient drift motions needs to be solved in this regard since the mode growth rate and mode structure depend on the toroidal drifts and magnetic configuration. Models based on the collisional drift wave turbulence in a region with magnetic shear seem to catch the right trends.[7] However, collisionless plasma dynamics is more relevant to high temperature core plasmas in tokamak devices.

The impurity effects on ITG (or η_i) mode in collisionless plasmas are studied for shearless slab, shear slab and toroidal magnetic configurations in Ref. 8. Full hydrogen and impurity ion dynamics is taken into account and the ballooning representation is used to take care of the mode coupling introduced by the toroidicity of the tokamak plasmas. The same integral dispersion equation for toroidal drift modes is used to study the isotope effects on ITG and impurity driven modes as well as on plasma confinement in this work.

The remainder of this work is organized as follows. In Sec. II the integral dispersion equation, including second ion species, for toroidal plasmas is presented and explained for completeness. In Sec. III the numerical results for hydrogenic plasmas, with and without impurity species, are described. Both the ITG and impurity modes are studied in the former case. The correlation of these results with experimentally observed isotope scaling is discussed in Sec. IV. Section V is devoted to the conclusions of this study.

II Integral Dispersion Equation

The gyrokinetic integral equation[9] for the study of low frequency drift modes, such as the ITG mode, is extended to include impurity species in this section. The curvature and magnetic gradient effects $\omega_D(v_\perp^2, v_\parallel^2, \theta)$ of both hydrogenic and impurity ions are included. The ballooning representation is used so that the mode coupling due to the toroidal magnetic configuration of tokamak device is taken into account. The full ion transit $k_\parallel v_\parallel$ and finite Larmor radius effects are retained while the ion bouncing is neglected. Electron response is assumed to be adiabatic for simplicity. The integral dispersion equation derived in Ref. 9 is

easily written as follows after being extended to include second ion species,

$$[1+\tau_i(1-f_z)+\tau_z Z f_z]\,\widehat{\phi}(k)=\int_{-\infty}^{+\infty}\frac{dk'}{\sqrt{2\pi}}\,K(k,k')\widehat{\phi}(k')\ , \tag{1}$$

where

$$K(k,k')=-i\int_{-\infty}^{0}\omega_{*e}d\tau\,\sqrt{2}\,e^{-i\omega\tau}\left[(1-f_z)\frac{\exp\left[-\frac{(k'-k)^2}{4\lambda}\right]}{\sqrt{a}\,(1+a)\sqrt{\lambda}}\right.$$

$$\times\left\{\frac{\omega}{\omega_{*e}}\,\tau_i+L_{ei}-\frac{3}{2}\,\eta_i L_{ei}+\frac{2\eta_i L_{ei}}{(1+a)}\right.$$

$$\left.\left.\times\left[1-\frac{k_\perp^2+k'^2}{2(1+a)\tau_i}+\frac{k_\perp\,k'_\perp}{(1+a)\tau_i}\,\frac{I_1}{I_0}\right]+\frac{\eta_i L_{ei}(k-k')^2}{4a\lambda}\right\}\Gamma_0(k_\perp,k'_\perp)+\right.$$

$$+f_z\frac{\exp\left[-\frac{(k'-k)^2}{4\lambda_z}\right]}{\sqrt{a_z}\,(1+a_z)\sqrt{\lambda_z}}\left\{\frac{\omega}{\omega_{*e}}\,Z\tau_z+L_{ez}-\frac{3}{2}\,\eta_z L_{ez}+\frac{2\eta_z L_{ez}}{(1+a_z)}\right.$$

$$\left.\left.\times\left[1-\frac{(k_\perp^2+k'^2)\mu}{2(1+a_z)Z^2\tau_z}+\frac{k_\perp\,k'_\perp\mu}{(1+a_z)Z^2\tau_z}\,\frac{I_{1z}}{I_{0z}}\right]+\frac{\eta_z L_{ez}(k-k')^2}{4a_z\lambda_z}\right\}\Gamma_{0z}(k_\perp,k'_\perp)\right] \tag{2}$$

with

$$\lambda=\frac{\tau^2\omega_{*e}^2}{\tau_i a}\left(\frac{\widehat{s}}{q}\,\epsilon_n\right)^2\ ,\qquad \lambda_z=\frac{\tau^2\omega_{*e}^2}{\tau_z a_z\mu}\left(\frac{\widehat{s}}{q}\,\epsilon_n\right)^2\ ,$$

$$a=1+\frac{i2\epsilon_n}{\tau_i}\,\omega_{*e}\tau\left(\frac{(\widehat{s}+1)(\sin\theta-\sin\theta')-\widehat{s}(\theta\cos\theta-\theta'\cos\theta')}{(\theta-\theta')}\right)\ ,$$

$$a_z=1+\frac{i2\epsilon_n}{\tau_z Z}\,\omega_{*e}\tau\left(\frac{(\widehat{s}+1)(\sin\theta-\sin\theta')-\widehat{s}(\theta\cos\theta-\theta'\cos\theta')}{(\theta-\theta')}\right)\ ,$$

$$\theta=\frac{k}{\widehat{s}k_\theta}\ ,\qquad \theta'=\frac{k'}{\widehat{s}k_\theta}\ ,$$

$$\Gamma_0=I_0\left(\frac{k_\perp\,k'_\perp}{(1+a)\tau_i}\right)\exp\left[-(k_\perp^2+k'^2_\perp)/2\tau_i(1+a)\right]$$

$$\Gamma_{0z} = I_0\left(\frac{k_\perp k'_\perp \mu}{(1+a_z)\tau_z Z^2}\right)\exp\left[-(k_\perp^2 + k'^2_\perp)\mu/2Z^2\tau_z(1+a_z)\right] ,$$

$$k_\perp^2 = k_\theta^2 + k^2 , \qquad k'^2_\perp = k_\theta^2 + k'^2 ,$$

$$\epsilon_n = \frac{L_{ne}}{R} , \quad \eta_i = \frac{L_{ni}}{L_{Ti}} , \quad \eta_z = \frac{L_{nz}}{L_{Tz}} , \quad \tau_i = \frac{T_e}{T_i} , \quad \tau_z = \frac{T_e}{T_z} ,$$

$$f_z = \frac{Zn_{0z}}{n_{0e}} , \quad \mu = \frac{m_z}{m_i} , \quad L_{ei} = \frac{L_{ne}}{L_{ni}} , \quad L_{ez} = \frac{L_{ne}}{L_{nz}} .$$

k, k' and k_θ are normalized to $\rho_i^{-1} = \Omega_i/v_{ti} = eB/c\sqrt{2T_i m_i}$ and x to ρ_i, and $I_j(j = 0, 1)$ is the modified Bessel function of order j. The symbols with subscript "i" or without stand for the primary ion species (hydrogenic ions) while that with "z" and "e" for the second and electrons, respectively, in Eqs. (1)–(2) and the expressions afterwards. In addition, all the symbols have their usual meanings such as: the L_n's are the density scale lengths, L_T's the temperature scale lengths, q the safety factor, $\hat{s} = rdq/qdr$ the magnetic shear, and ω_{*e} the electron diamagnetic frequency. Z is the charge number of impurity ions, m's and T's are the ion mass and temperature, respectively. The derivation of the equation is given in detail in Ref. 9 and not repeated here.

It has to be mentioned before starting to solve Eq. (1) that not all the parameters are independent. This is because the quasineutrality condition holds in the plasmas studied here. This condition requires that

$$L_{ei} = \frac{1 - f_z L_{ez}}{1 - f_z} , \tag{3}$$

and therefore

$$\eta_z = \frac{\eta_i\left(\frac{L_{ni}}{L_{ne}} - f_z\right)}{1 - f_z} , \tag{4}$$

under the assumption $T_i(r) = T_z(r)$.

III Numerical Results

Equation (1) has to be solved numerically and special attention must be paid to the logarithmic singularity at $\tau = 0$ when $k = k'$.[9] The numerical methods for solving such a Fredholm integral equation of the second kind are standard and well documented,[9] so will not be repeated in this work.

The following reference parameters are used in this study unless otherwise stated: $\eta_i = \eta_z = 3.9$, $f_z = 0.2$, $\hat{s} = 0.83$, $q = 1.5$, $\epsilon_n = 0.56$, $\tau_i = \tau_z = 1$, $L_{ei} = L_{ez} = 1$.

A. ITG mode in pure hydrogenic plasmas

The ITG mode in pure hydrogenic (H, D, T or their mixture) plasmas is studied first to show the isotope effects on the mode. The normalized mode growth rate as a function of $k_\theta \rho_H$ is given in Fig. 1, where $\rho_H = c\left(2T_i m_i\right)^{1/2}/eB$ is the hydrogen ion Larmor radius. The mode growth rate is normalized to $\omega_{*e}/k_\theta\rho_H = \sqrt{\tau/2}c_{sH}/L_n$ so that the normalized growth rate is independent of the poloidal mode number k_θ which is the variable on the absissa axis. This is the right way to present the results and to perform comparisons since the same normalization is taken for different ion species so that the numbers shown in the figures are comparable.

The analysis makes it very clear that ITG mode has the highest maximum growth rate and the widest k_θ range where the mode is unstable in a hydrogen plasma. Tritium plasma which has the lowest maximum growth rate and the narrowest unstable k_θ range is the most stable. A deuterium plasma is in between. The stability of ITG mode in a half and half D-T plasma is just between deuterium and tritium plasmas, and the same for the half and half H-D plasmas. It is easy to figure out that the maximum growth rates $\gamma_{\max\, H} : \gamma_{\max\, D} : \gamma_{\max\, T} = 1 : 1/\sqrt{2} : 1/\sqrt{3}$, i.e. the maximum growth rate of the mode is inversely proportional to the square root of the ion mass number. This relation holds for

D-T and H-D mixing plasmas if an average mass number is used. The correlation of these results with isotope scaling of energy confinement in tokamak plasmas will be discussed in Sec. IV.

B. ITG mode in plasmas with impurities

Real plasmas in tokamak devices are not pure hydrogen plasmas. Instead there are lower densities of higher Z elements called impurities in such plasmas. A second ion species (m_z, Z, n_z) is now introduced in order to study the isotope effects on ITG mode in the presence of impurities. Two kinds of impurities, carbon and helium, are considered. Shown in Fig. 2 is the normalized mode growth rate as a function of poloidal wavenumber. The same normalization as that in Fig. 1 is used. In both carbon and helium cases the impurity concentration $f_z = Zn_z/n_e = 0.2$ is used, corresponding to $Z_{\rm eff} = 2$ with carbon and $Z_{\rm eff} = 1.2$ with helium, respectively. Again, the mode has the highest maximum growth rate in a hydrogen plasma, the lowest in a tritium, and the intermediate in a deuterium plasma. In addition, the mode growth rate in plasmas with carbon is lower than that with helium when the primary ions are the same kind (H, D, or T).

C. Impurity Mode

An impurity mode can be driven unstable when there is a second ion species in the plasma with its density peak opposite to the primary ion and electron densities.[10] With opposing density gradients, no ion temperature gradient is needed to drive this instability. We choose $\eta_i = \eta_z = 0$, $L_{ne} = -2L_{nz}$, $\hat{s} = 1$, $q = 2.5$, $\epsilon_n = 0.3$. The parameter $L_{ei} = L_{ne}/L_{ni}$ is calculated from Eq. (3). Oxygen is considered to be the impurity in hydrogen, deuterium or tritium plasmas. Shown in Fig. 3 is the mode growth rate as a function of the wavenumber in the poloidal direction. Two impurity concentrations of $f_z = 0.2$ and 0.3 ($Z_{\rm eff} = 2.4$ and 3.1) are studied in Figs. 3(a) and (b), respectively. In these two cases the mode growth

rate is the highest in a hydrogen plasma, the lowest in a tritium, and the intermediate in a deuterium plasma. In addition, the mode has the widest range of unstable k_θ in a hydrogen plasma, narrowest in a tritium, and the intermediate in a deuterium plasma, just as the ITG mode does. The mode growth rate increases with increasing impurity concentration for the same discharge gas in the range of parameters studied here.

IV Discussion

It is widely believed that the ITG mode is a plausible candidate responsible for the anomalous energy transport in tokamak plasmas. There has been an effort to explain experimental observations with ITG theories.[11] As one part of such an effort it is natural to try to find some relationship between the ITG mode features and the experimental observations on the isotope scaling. The mixing length argument, $\chi \simeq \gamma \Delta_r^2$, is usually used to calculate the thermal diffusivity χ, where γ is the linear mode growth rate and Δ_r is the mode correlation length in the radial direction. The conventional estimate identifies Δ_r with the mode width of a single helicity harmonic and takes $\Delta_r \sim k_\theta^{-1}$ on the order of the ion gyro-radius. Such an estimation gives rise to two important discrepancies with the experiments. The first is the radial profile of $\chi(r)$ as discussed by Beklemishev and Horton[12] and the second is the isotope scaling of the energy diffusion coefficient.

Recent toroidal particle simulations show that the radial correlation length is longer than and does not scale directly with $1/k_\theta$.[13] Indeed, an electrostatic perturbation is a superposition of different poloidal harmonics in a tokamak plasma. The neighboring harmonics are coupled and overlapped due to the toroidicity of the configuration. The mode correlation length Δ_r may be much longer than and independent of the mode width of a single harmonic if such coupling and overlapping are strong. Based on such physical considerations, theoretical studies have shown that the radial correlation length can be a function of plasma parameters, independent of and much longer than the mode width of a single helicity har-

monic.[14, 15] In addition, density fluctuation measurements in tokamak plasmas indicate that the wavenumber spectrum $S(k_r)$ peaks at $k_r = 0$ while the spectrum $S(k_\theta)$ peaks at $k_\theta \neq 0$.[16] However, finding out the proper formula for Δ_r is still a challenge to plasma physicists and is beyond the scope of this work. Even with these uncertainties in the scaling of the radial correlation length with the ion mass, the growth rate controls the driving force for the turbulent energy.

It is qualitatively demonstrated in Sec. III that the ITG mode has the highest growth rate and widest unstable k_θ spectrum in a hydrogen plasma, the lowest growth rate and narrowest k_θ spectrum in a tritium plasm, and the intermediate growth rate in a deuterium plasma. Some attempts are made to relate these results with the isotope scaling experimentally observed. In doing so we assume that the correlation time is determined by the single harmonic with the maximum growth rate and that the correlation length is independent of the mode width of each single harmonic and determined by equilibrium plasma parameters. Then the maximum growth rate of the ITG mode has an isotope scaling similar to that obtained from experimental data. Shown in Fig. 4 is the maximum growth rate from Figs. 1–2 as a function of effective mass number

$$M_{\rm eff} = (1 - f_z)A_i + f_z A_z \ , \tag{5}$$

where A_i and A_z are the mass number for hydrogenic ions and impurity ions, respectively, and the same normalization as that in Figs. 1 and 2 is used for $\gamma_{\rm max}$. The solid line is the curve of $\gamma_{\rm max} \propto M_{\rm eff}^{-0.5}$ matching the calculated value at the point $M_{\rm eff} = 1$. Considering that the parameter values of $\eta_i, q, \hat{s}, \epsilon_n$, and f_z used in the calculation are chosen randomly from those close to experimental observations, the $M_{\rm eff}^{-0.5}$ parameterization of $\gamma_{\rm max}$ is considered good.

The $\gamma_{\rm max}$ versus $M_{\rm eff}$ dependence shown in Fig. 5 is the same as that in Fig. 4 but for the impurity driven mode. In this case the fitting with $M^{-0.5}$, with M being the mass number

of the hydrogenic ions, is also good. Our attempt to fit these data by one curve with the effective mass number as that for the ITG mode failed, indicating that $Z_{\rm eff}$ is important for the maximum growth rate of the impurity mode. Taking the influence of $Z_{\rm eff}$ into account, we find that $\gamma_{\rm max} \propto M^{-0.5} Z_{\rm eff}^{1.5}$ fits the data given in Fig. 5 reasonably good. Both ITG and impurity modes have approximately the same isotope scaling $\gamma_{\rm max} \propto M^{-0.5}$. Besides, the impurity mode has the scaling $\gamma_{\rm max} \propto Z_{\rm eff}^{1.5}$ which may provide a way to distinguish impurity mode dominated transport from the ITG mode induced transport if the diffusion

V Conclusions

The integral toroidal gyrokinetic dispersion equation is extended to include a second ion species. The ion temperature gradient driven mode (or η_i mode) is studied in hydrogen, deuterium or tritium plasmas with or without the presence of impurity ions. It is shown that the ITG mode has the highest growth rate and the widest unstable k_θ spectrum in a hydrogen plasma, the lowest growth rate and narrowest k_θ spectrum in a tritium plasma, and an intermediate growth rate in a deuterium plasma. The maximum growth rate of the mode with respect to the poloidal mode number k_θ is found to scale as $\gamma_{\rm max} \propto M_{\rm eff}^{-0.5}$ with $M_{\rm eff}$ being the effective ion mass number defined in Eq. (5). This scaling is in reasonable agreement with the experimental observations if the mixing length estimation for the plasma energy transport is used, under the assumption that the correlation time is inversely proportional to the maximum growth rate of the mode, and that the correlation length is independent of each single harmonic mode width.

The impurity driven mode is studied in hydrogen, deuterium or tritium plasmas without the temperature gradient of either the primary or the impurity ion species. The mode growth rate has the same feature as that of the η_i mode: the highest growth rate and the widest unstable k_θ spectrum in a hydrogen plasma, the lowest growth rate and narrowest k_θ spectrum in a tritium plasma, and an intermediate growth rate in a deuterium plasma. The

maximum mode growth rate scales as $\gamma_{max} \propto M^{-0.5}$ for the same impurity concentration f_z, where M is the mass number of the primary ion species. Taking Z_{eff} influence into account, $\gamma_{max} \propto M^{-0.5} Z_{eff}^{1.5}$ fits the numerical data reasonably well. The scaling $\gamma_{max} \propto Z_{eff}^{1.5}$ of the impurity mode is one of the major differences from the ITG mode, that may provide the distinction between the ITG mode dominated and impurity mode dominated plasma transports if the diffusion induced by the impurity mode is assumed to be proportional to the maximum growth rate and independent of the mode width of a single helicity harmonic component due to the toroidal mode structures.

It has to be pointed out that the isotope scaling discussed in this study only works for fixed plasma parameters such as density and temperature gradients, magnetic and velocity shears, magnetic curvature and safety factor. This means that the isotope scaling $\tau_E \propto M_{eff}^{0.5}$ proposed in this work only holds for discharges with exactly the same plasma parameter profiles in different working gases. The profile of those plasma parameters, however, usually change from one working gas to another in experiment. As a result, it is not surprising to find that weak or even no isotope effects are observed for some plasmas in certain discharge modes as, for example, the L-mode plasmas on DIII-D with neutral beam injection.[17]

Acknowledgments

This work was supported by the U.S. Department of Energy contract #DE-FG05-80ET-53088.

References

[1]R.J. Goldston, Plasma Phys. Contr. Fusion **26**, 87 (1984).

[2]S.M. Kaye, Phys. Fluids **28**, 2327 (1985).

[3]M. Bessenrodt-Weberpals, F. Wagner, ASDEX Team, Nucl. Fusion **33**, 1205 (1993).

[4]R.R. Dominguez, Nucl. Fusion **31**, 2063 (1991).

[5]B. Coppi, in Plasma Phys. and Contr. Nucl. Fusion Research 1990 (Proc. 13th Int. Conf. Washington, DC. 1990) vol. 2, IAEA, Vienna 413 (1991).

[6]B. Coppi, P. Detragiache, S. Migliuolo, M. Nassi, B. Rogers, L. Sugiyama and L. Zakharov, in Plasma Phys. and Contr. Nucl. Fusion Research 1990 (Proc. 14th Int. Conf. Wurzhburg, 1992) vol. 2, IAEA, Vienna 131 (1993).

[7]B.D. Scott, Phys. Fluids B **4**, 2468 (1992).

[8]J.Q. Dong, W. Horton, and X.N. Su, in Ion Temperature Gradient-Driven TurbulentTransport, Eds. W. Horton, A. Wootton, and M. Wakatani, (AIP Conference Proceedings, January, 1994), p. 366.

[9]J.Q. Dong, W. Horton, and J.Y. Kim, Phys. Fluids B **4**, 1867 (1992).

[10]B. Coppi, H.P. Furth, M.N. Rosenbluth, and R.Z. Sagdeev, Phys. Rev. Lett. **17**, 337 (1966).

[11]W. Horton, D. Lindberg, J.Y. Kim, J.Q. Dong, G.W. Hammett, S.D. Scott, and M.C. Zarnstorff, Phys. Fluids B **4**, 952 (1992).

[12]A.D. Beklemishev and W. Horton, Phys. Fluids B **4**, 2176 (1992).

[13]M.J. Lebrun, T. Tajima, M.G. Gray, G. Furnish, and W. Horton, Phys. Fluids B **5**, 752 (1993); and T. Tajima, Y. Kishimoto, M.J. LeBrun, M.G. Gray, J.Y. Kim, W. Horton, H.V. Wong, and M. Kotschenreuther, in Ion Temperature Gradient-Driven Turbulent Transport, Eds. W. Horton, A. Wootton, and M. Wakatani, (AIP Conference Proceedings, 1994), p. 255.

[14]J.W. Connor, J.B. Taylor, and H.R. Welson, Phys. Rev. Lett. **70**, 1803 (1993); and J.B. Taylor, J.W. Connor, and H.R. Wilson, Plasma Phys. Contr. Fusion **35**, 1063 (1993).

[15]F. Romanelli and F. Zonca, Phys. Fluids B **5**, 4081 (1993).

[16]R.J. Fonk, G. Cosby, R.D. Durst, S.F. Paul, N. Bretz, S. Scott, E. Synakowski, and G. Taylor, Phys. Rev. Lett. **70**, 3736 (1993).

[17]D.P. Schissel, K.H. Burrell, J.C. DeBoo, R.J. Groebner, A.G. Kellman, N. Ohyabu, T.H. Osborne, M. Shimada, R.T. Snider, R.D. Stambaugh, T.S. Taylor, and the DIII-D Research Team, Nucl. Fusion **29**, 185 (1989).

Figure Captions

1. Normalized ITG mode growth rate versus poloidal wavenumber for pure hydrogenic plasmas. In all figures the growth rate is in unit of $T_e/\sqrt{2T_i m_H}L_n$, and the wavenumber is in unit of $eB/c\sqrt{2T_i m_H}$.

2. Normalized ITG mode growth rate versus poloidal wavenumber for plasmas with impurities, the solid lines are for helium impurity and the dotted lines for carbon impurity.

3. Normalized impurity mode growth rate versus poloidal wavenumber, (a) $f_z = 0.2$, and (b) $f_z = 0.3$.

4. The maximum growth rate of the ITG mode versus the effective mass number for the calculations given in Figs. 1 and 2. The solid line is $\gamma_{max} \sim M_{eff}^{-0.5}$ fitting.

5. The maximum growth rate of the impurity mode versus the mass number of the primary ions for the calculations given in Fig. 3. The lines are $\gamma_{max} \sim M^{-0.5}$ fitting, the solid line is for $f_z = 0.2$ and the dash-dotted line for $f_z = 0.3$.

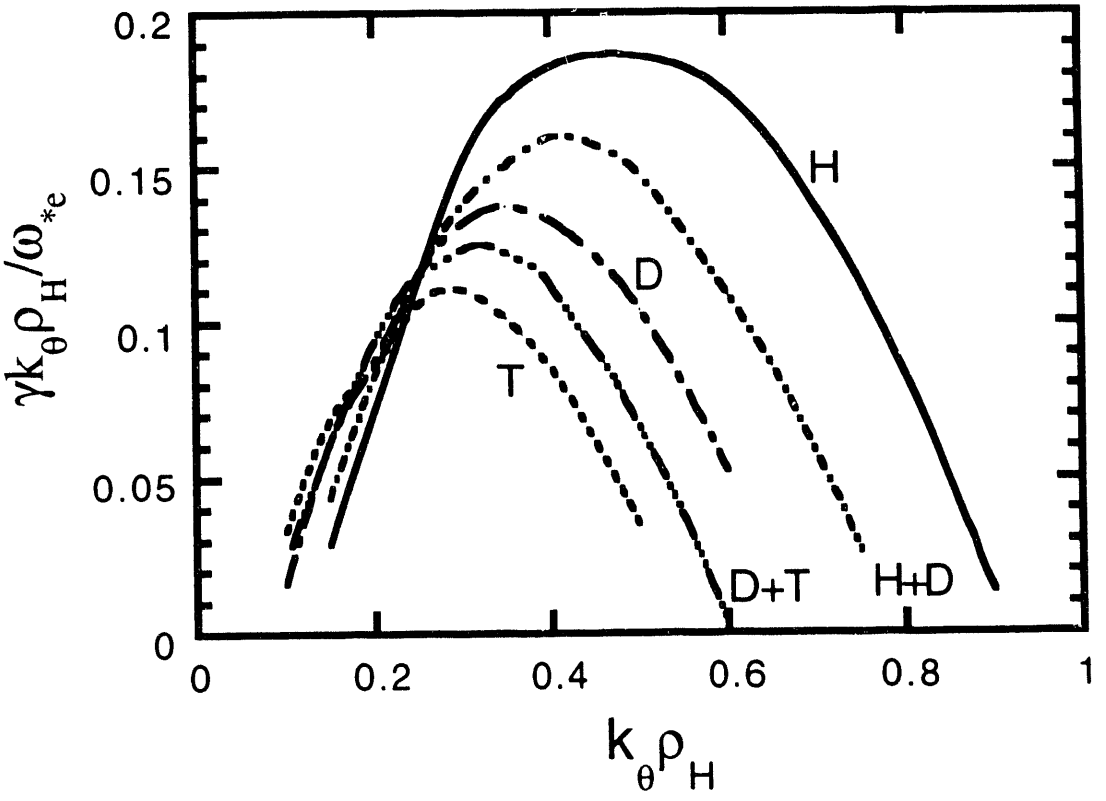
0.2
0.15
0.1
0.05
0
0
0.2
0.4
0.6
0.8
1
$\gamma k_\theta \rho_H / \omega_{*e}$
$k_\theta \rho_H$
H
D
T
D+T
H+D

Fig.1

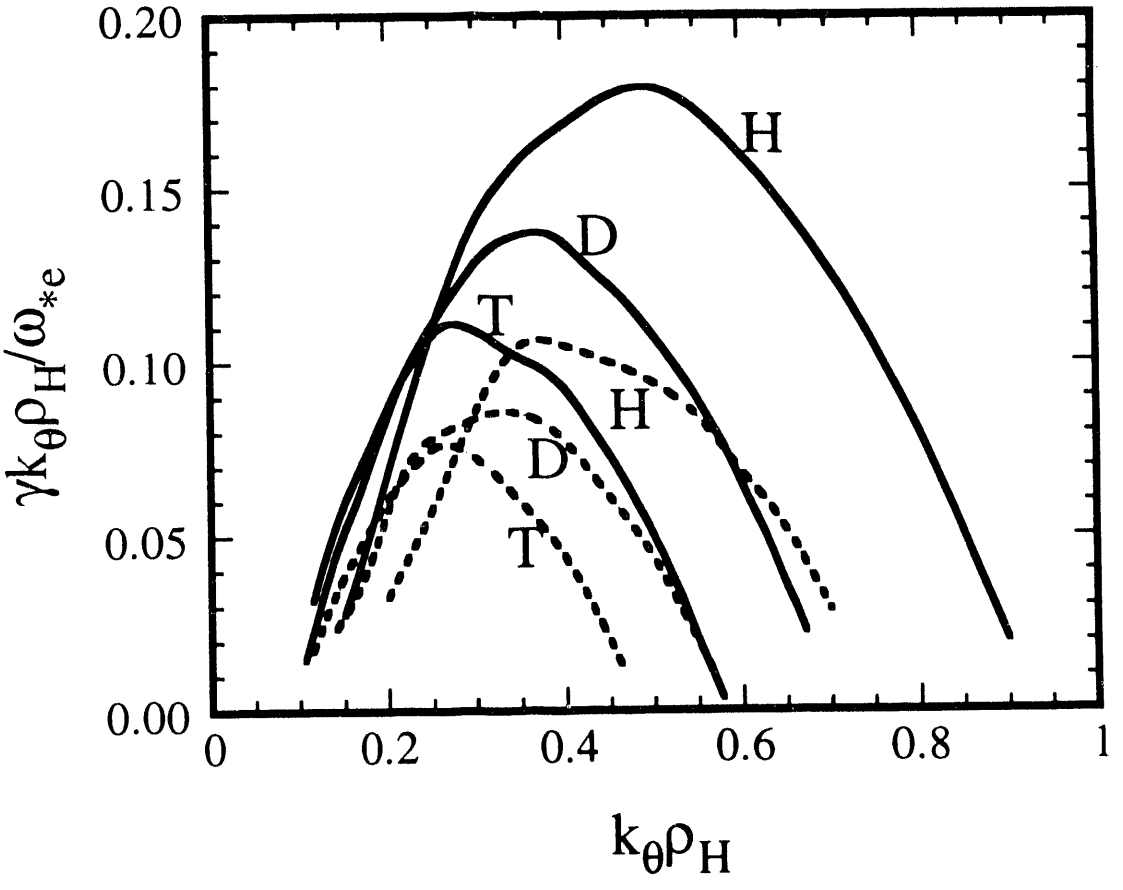
0.20
0.15
0.10
0.05
0.00
0
0.2
0.4
0.6
0.8
1
H
D
T
H
D
T
$\gamma k_\theta \rho_H / \omega_{*e}$
$k_\theta \rho_H$

Fig. 2

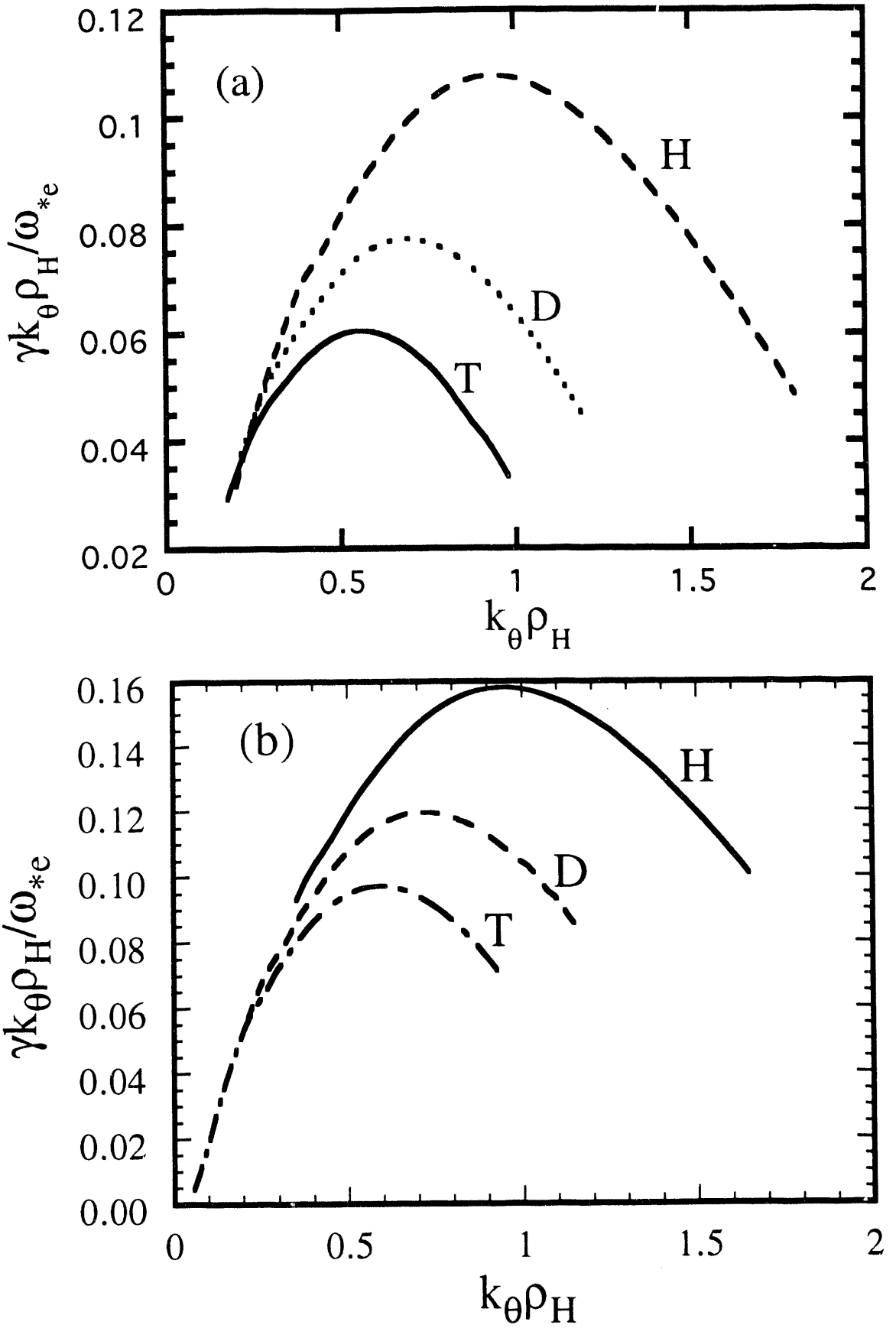
(a)
H
D
T
0.12
0.1
0.08
0.06
0.04
0.02
0
0.5
1
1.5
2
$\gamma k_\theta \rho_H / \omega_{*e}$
$k_\theta \rho_H$
(b)
H
D
T
0.16
0.14
0.12
0.10
0.08
0.06
0.04
0.02
0.00
0
0.5
1
1.5
2
$\gamma k_\theta \rho_H / \omega_{*e}$
$k_\theta \rho_H$

Fig. 3

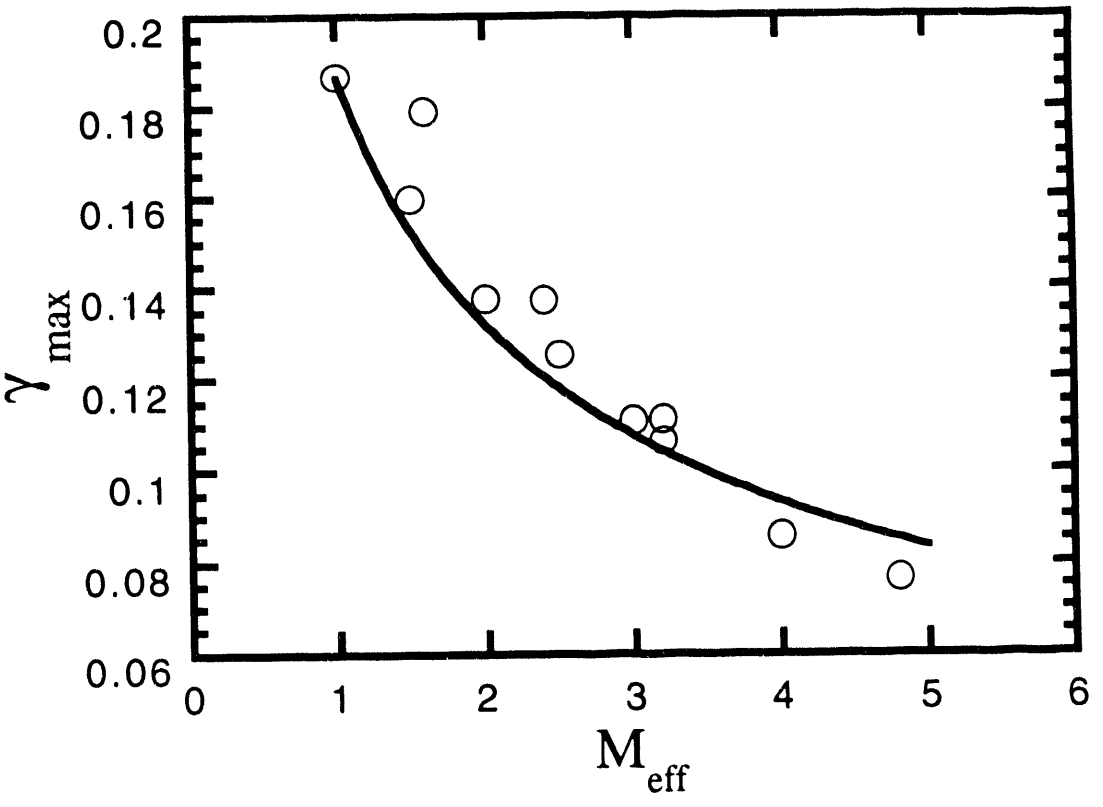

Fig.4

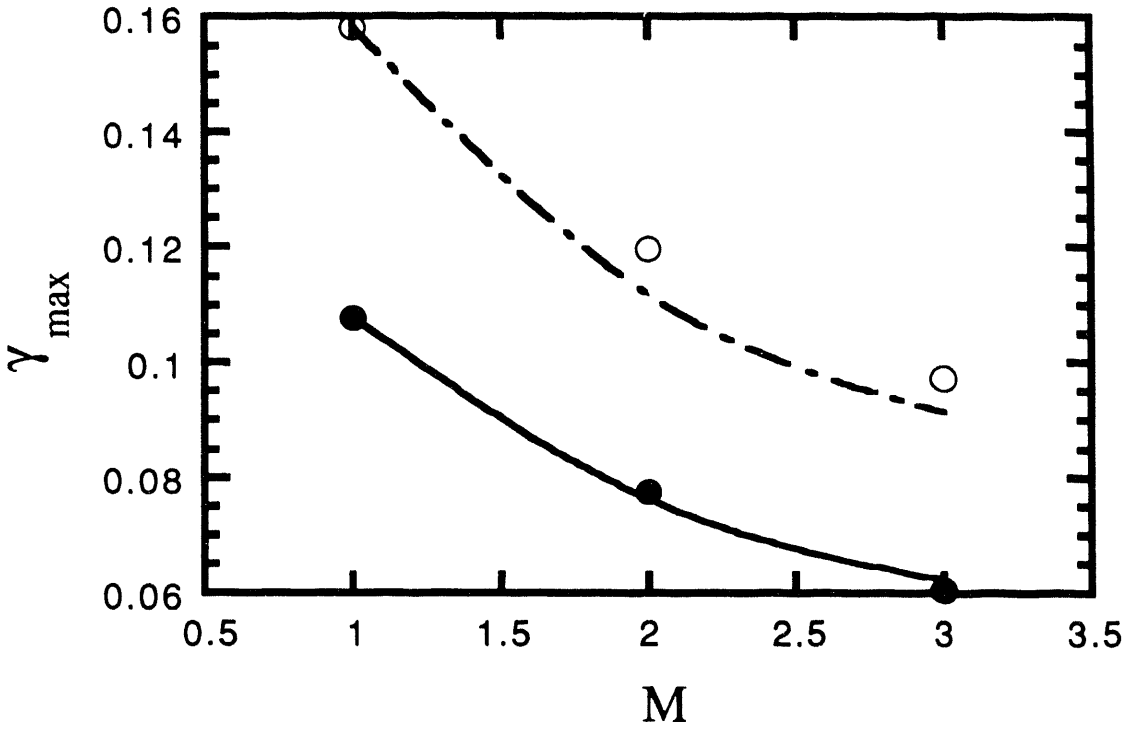

Fig. 5

DATE FILMED

7/1/94

END